Chemical and Process Engineering Research
ISSN 2224-7467 (Paper) ISSN 2225-0913 (Online)
Vol.33, 2015

Numerical Investigation of the Effect of Reactor Severity on Biomass Pyrolysis Characteristics in Thermally Thick Regime

Pious O. Okekunle

Department of Mechanical Engineering, Faculty of Engineering and Technology,
Ladoke Akintola University of Technology, P.M.B. 4000, Ogbomoso, Oyo state, Nigeria.
Author's email address: pookekunle@lautech.edu.ng

Abstract

Effect of reactor peak temperature on biomass pyrolysis in thermally thick regime with a constant heating rate of 30 K/s, reactor pressure of 1 atm and reactor peak temperature ranging from 500 to 1000 ^{o}C in a fixed-bed reactor has been numerically investigated. Wood cylinders ($\rho = 400\ kg/m^3$, $\emptyset\ 10\ mm$ and length $20\ mm$) were modeled as two-dimensional porous solids. Transport equations, solid mass conservation equations, intra-particle pressure generation equation and energy conservation equation were coupled and simultaneously solved to simulate the pyrolysis process. First order Euler Implicit Method (EIM) was used to solve the solid mass conservation equations. The transport, energy conservation and intra-particle pressure generation equations were discretized by Finite Volume Method (FVM). The generated set of linear equations was solved by Tri-Diagonal Matrix Algorithm (TDMA). Intra-particle fluid flow velocity was estimated by Darcy's law. Results showed that increase in reactor temperature from 500 to 600 ^{o}C and from 600 ^{o}C to 700 ^{o}C favoured primary tar intra-particle secondary reactions, causing corresponding increase in the release rate and yield of gas and secondary tar. Increase in reactor temperature beyond 700 ^{o}C had no significant influence on primary tar intra-particle secondary reactions and on the release rates and yields of volatiles and primary tar. Char yield, however, decreased continually with increase in reactor temperature. The highest gas yield (50.10%) was obtained at 700 ^{o}C, primary tar yield (33.91%) at 500 ^{o}C and char yield (14.79%) at 500 ^{o}C.

Keywords: Biomass, pyrolysis, intra-particle secondary reactions, thermally thin regime

1. Introduction

Many biomass commercial thermochemical conversion systems use sample sizes and heating rates that cause both spatial and temporal gradients of temperature, pressure and volatile species concentration within biomass samples during pyrolysis. These intra-sample gradients will most likely influence various physical phenomena and intra-particle secondary reactions kinetics, thereby affecting volatiles evolution, compositions and total yields. Exploring the great potential of these thermochemical conversion systems therefore requires some adequate understanding of the influence of process parameters in a situation where all these occur. Pyrolysis, being a viable means of obtaining bio-fuels for supplementing or replacing fossils, has been receiving a lot of attention. Wood has been considered has one of the most reliable materials that will make biomass thermochemical conversion technology a veritable source of energy for sustainable development in the nearest future. Many researchers have attempted to explain the mechanism of wood pyrolysis both in thermally thin and thermally thick regimes [1-8]. Some others also have studied the behaviour of cellulose pyrolysis under various process conditions [9-13]. Some of these studies were undertaken with sample sizes ranging from 0 to 1 mm where intra-particle physical phenomena are too fast and volatile secondary reactions not significant. In such cases, results obtained were inadequate to discuss various scenarios in thermally thick regime. Previous research efforts have shown that pyrolysis in thermally thin and thermally thick regimes under the same process conditions will have different release rates and yields of volatile and liquid products [14-17]. Char yield may also be affected. In this study, effects of reactor final temperature on biomass pyrolysis characteristics in thermally thick regime were numerically investigated. The weight loss history, volatiles and liquid release rates

and yields, and char yield at various reactor temperatures are presented. An attempt was also made to explain the implications of varying reactor final temperature on intra-particle secondary reactions in this regime.

2. Pyrolysis Mechanism

Figure 1 shows the structure of the pyrolysis mechanism adopted in this study. A detailed explanation on the development of this mechanism has been reported in our earlier research works [18, 19]. As shown in the figure, wood first decomposes by three endothermic competing primary reactions to form gas, primary tar and intermediate solid. The primary tar undergoes secondary reactions to yield more gas and char. The intermediate solid is further transformed into char by a strong exothermic reaction as shown in the figure. Reaction rates were assumed to follow Arrhenius expression of the form; $k_i = A_i \exp\left({}^{-E_i}/_{RT}\right)$. The chemical kinetic (*A* and *E*) and thermodynamic (*a* and *b*) parameters are as given in one of our previous works [19].

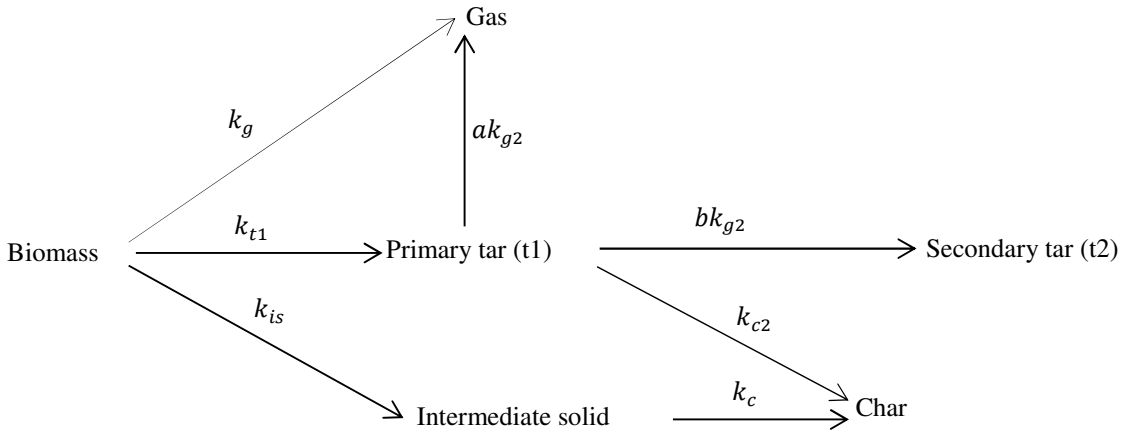

Figure 1: Schematic illustration of pyrolysis mechanism

3. Numerical simulation

The governing equations, model assumptions and numerical procedures in this study are already given in our previous studies [18, 19, 20]. Hence, fundamental governing equations will only be set out.

3.1 Solid mass conservation equations

The instantaneous mass balance of the pyrolyzing solid comprises three endothermic consumption terms yielding gas, primary tar and intermediate solid:

$$\frac{\partial \rho_s}{\partial t} = -(k_g + k_t + k_{is})\rho_s \quad (1)$$

The intermediate solid instantaneous mass balance equation (equation (2)) contains two terms, one for the conversion of the virgin solid to intermediate solid and the other from exothermic decomposition of intermediate solid to yield char, given as

$$\frac{\partial \rho_{is}}{\partial t} = k_{is}\rho_s - k_c\rho_{is} \quad (2)$$

Also, the char instantaneous mass balance equation (equation(3)) contains two terms, one from the exothermic decomposition of intermediate solid and the other from primary tar secondary reaction to yield char, given as

$$\frac{\partial \rho_c}{\partial t} = k_c\rho_{is} + k_{c2}\rho_t \quad (3)$$

3.2 Mass conservation equations of gas phase components

Mass conservation equations for all gas phase components are expressed by two-dimensional cylindrical coordinate system consisting of both temporal and spatial gradients and source terms, given by

Ar: $\frac{\partial(\varepsilon\rho_{Ar})}{\partial t} + \frac{\partial(\rho_{Ar}U)}{\partial z} + \frac{1}{r}\frac{\partial(r\rho_{Ar}V)}{\partial r} = S_{Ar},$ (4)

Gas: $\frac{\partial(\varepsilon\rho_{g})}{\partial t} + \frac{\partial(\rho_{g}U)}{\partial z} + \frac{1}{r}\frac{\partial(r\rho_{g}V)}{\partial r} = S_{g},$ (5)

Primary tar : $\frac{\partial(\varepsilon\rho_{t1})}{\partial t} + \frac{\partial(\rho_{t1}U)}{\partial z} + \frac{1}{r}\frac{\partial(r\rho_{t1}V)}{\partial r} = S_{t1},$ (6)

Secondary tar: $\frac{\partial(\varepsilon\rho_{t2})}{\partial t} + \frac{\partial(\rho_{t2}U)}{\partial z} + \frac{1}{r}\frac{\partial(r\rho_{t2}V)}{\partial r} = S_{t2}$ (7)

S_{Ar} , S_g, S_{t1} and S_{t2} are the source terms for the carrier gas (argon), gas, primary tar and secondary tar respectively, and are given by

$S_{Ar} = 0$ (8)

$S_g = k_g\rho_s + \varepsilon k_{g2}\rho_{t1}$ (9)

$S_{t1} = k_t\rho_s - \varepsilon[k_{c2} + (a+b)k_{g2}]\rho_{t1}$ (10)

$S_{t2} = \varepsilon b k_{g2}\rho_{t1}$ (11)

Intra-particle tar and gas transport velocity was estimated by Darcy's law, expressed as

$U = -\frac{B}{\mu}\left(\frac{\partial P}{\partial z}\right)$ (12)

$V = -\frac{B}{\mu}\left(\frac{\partial P}{\partial r}\right)$ (13)

where B and μ are respectively the charring biomass solid permeability and kinematic viscosity. Porosity,ε, is expressed as

$\varepsilon = 1 - \frac{\rho_{s,sum}}{\rho_{w,0}}(1 - \varepsilon_{w,0})$ (14)

where $\varepsilon_{w,0}, \rho_{s,sum}$ and $\rho_{w,0}$ are the initial porosity of wood, the sum of solid mass density and initial wood density, respectively. The permeability, B, of the charring biomass is expressed as a linear interpolation between the solid phase components, given as

$B = (1 - \eta)B_w + \eta B_c$ (15)

where η is the degree of pyrolysis and is defined as

$\eta = 1 - \frac{\rho_s + \rho_{is}}{\rho_{w,0}}$ (16)

3.3 Energy conservation equation

The energy conservation equation is given as

$$\left(C_{p,w}\rho_s + C_{p,w}\rho_{is} + C_{p,c}\rho_c + \varepsilon C_{p,t}\rho_{t1} + \varepsilon C_{p,t}\rho_{t2} + \varepsilon C_{p,g}\rho_g\right)\frac{\partial T}{\partial t} = \frac{\partial}{\partial z}\left(k_{eff(z)}\frac{\partial T}{\partial z}\right) + \frac{1}{r}\frac{\partial}{\partial r}\left(rk_{eff(r)}\frac{\partial T}{\partial r}\right) - l_c\Delta h_c - \sum_{i=g,t1,is} m_i\Delta h_i - \varepsilon\sum_{i=g2,t2,c2} n_i\Delta h_i \quad (17)$$

where

$$l_c = A_c \exp(-E_c/RT)\,\rho_{is} \quad (18)$$

$$m_i = A_i \exp(-E_i/RT)\,\rho_s \quad i = g, t1, is \quad (19)$$

$$n_i = A_i \exp(-E_i/RT)\,\rho_{t1} \quad i = g2, t2, c2 \quad (20)$$

The thermo-physical properties of the wood sample are as given in our previous study [14].

3.4 Pressure evolution

The total pressure is the sum of the partial pressures of the inert gas (argon), gas and secondary tar from the pyrolysis process. It is given as

$$P = P_{Ar} + P_{t2} + P_g;\;\; P_i = \frac{\rho_i RT}{M_i} \qquad (i = Ar, t2, g) \quad (21)$$

where M_i and R are the molecular weight of each gaseous species and universal gas constant, respectively. Combining equations (4), (5), (7), (12), (13) and (21), intra-particle pressure equation was obtained as

$$\frac{\partial}{\partial t}\left(\varepsilon\frac{P}{T}\right) - \frac{\partial}{\partial r}\left[\frac{BP}{\mu T}\left(\frac{\partial P}{\partial z}\right)\right] - \frac{1}{r}\frac{\partial}{\partial r}\left[r\frac{BP}{\mu T}\left(\frac{\partial P}{\partial r}\right)\right] = \frac{R}{M_{t2}}S_{t2} + \frac{R}{M_g}S_g \quad (22)$$

3.5 Numerical Procedure

Wood cylinders were modeled as two-dimensional porous solids. Wood pores were assumed to be initially filled with argon. As the solid was pyrolyzed, tar and gas were formed while argon was displaced to the outer region without participating in the pyrolysis reaction. The solid mass conservation equations (eqs (1) – (3)) were solved by first-order Euler Implicit Method. The mass conservation equations for argon, primary tar, gas and secondary tar (eqs (4) – (7)), energy conservation equation (eq. (17)) and the pressure equation (eq. (22)) were discretized using Finite Volume Method (FVM). Hybrid differencing scheme was adopted for the convective terms. First-order fully implicit scheme was used for the time integral with time step of 0.005 s. The detailed numerical procedure and calculation domain have been given somewhere else [18]. Model assumptions have also been given previously [20].

4. Results and discussion

4.1 Peak temperature effect on weight loss history

Figure 2 shows the weight loss history of the pyrolyzing sample at different reactor peak temperatures. As shown in the figure, at the initial stage, the heat absorbed by the sample was used in heating it and raising its temperature to a level where active disintegration reactions commenced. During sample heat-up, some water molecules trapped within the sample would evaporate. This would reduce the moisture content in the pyrolyzing sample before the initiation of its conversion. For the peak temperature range considered, particle heat-up continued until 10 s after which active disintegration of the sample began. As would be expected, the rate of sample weight loss increased with increase in reactor peak temperature. This implies that the rate of sample conversion to various products increased with increase in reactor peak temperature. From the figure, it can also be seen that the fraction of the solid weight remaining when active disintegration of the sample no longer took place decreased with increase in reactor peak temperature. This observation suggests that char yield decreased

with increase in reactor peak temperature while gas and tar production from primary pyrolysis were favoured. As would be expected, increase in temperature shortened the length of time required for the conversion of the pyrolyzing sample into various products. As shown in the figure, increase in temperature was accompanied with reduction in the fraction of the solid residue after pyrolysis.

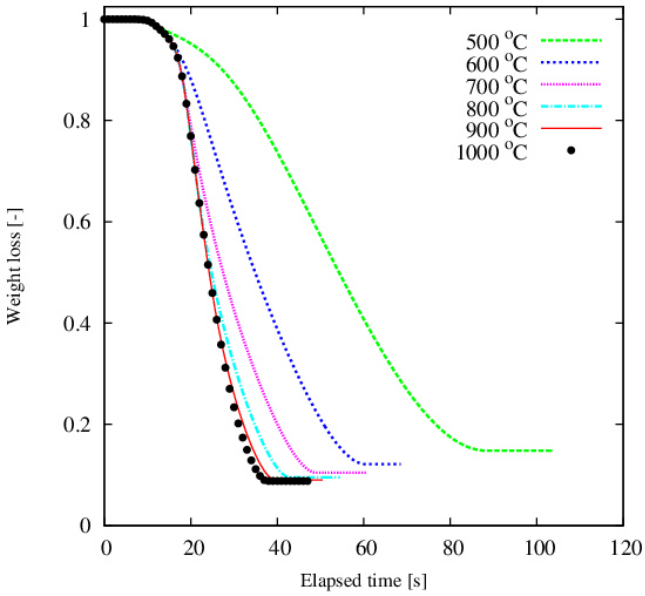

Figure 2: Weight loss history at different reactor peak temperatures

4.2 Effect on primary tar production

Figure 3 shows the rate of primary tar production at various pyrolysis temperatures. From the figure, virtually at all reactor temperatures, tar production rate was very low until about 10 s when it began to rise. As the reactor temperature increased from 500 to 600 ^{o}C, the rate of primary tar production increased until about 15 s when the peak was reached. Beyond this time, primary tar evolution rate began to fall until it approached zero and became seemingly constant throughout the pyrolysis process. A further increase in reactor temperature from 600 to 700 ^{o}C resulted in more increase in the rate of primary tar production, the peak of primary tar production profile being at about 15 s also but much higher than that at 600 ^{o}C. As reactor temperature increased beyond 700 ^{o}C, primary tar production rate appeared unchanged and the profiles of tar production from 700 ^{o}C to 1000 ^{o}C were the same. This suggests the possibility of a certain threshold during pyrolysis above which increase in reactor temperature no longer influenced the rates of primary reactions. It is also plausible that the sample being pyrolyzed has reached almost 100% conversion into various products before the reactor reached its final temperature (800 ^{o}C and above).

4.3 Effect on intra-particle secondary reactions products evolution

Figure 4 shows the rate of evolution of products from primary tar intra-particle secondary reactions at different reactor temperatures. From the figure, the profiles of the rates of release of secondary products are similar to the profiles of primary tar production rates at corresponding temperatures except that the peaks of the latter were higher than those of the former. As would be expected, increase in temperature from 500 to 600 ^{o}C and from 600 to 700 ^{o}C increased the rates of evolution of secondary products from primary tar intra-particle secondary reactions. From chemical kinetics, it is generally accepted that increase in temperature accelerates the rate of chemical reactions. Provided the sample being pyrolyzed has not been converted completely before reaching the final reactor temperature (between 500 and 700 ^{o}C), it should be expected that rise in reactor temperature will accelerate the rates of intra-particle secondary reactions thereby enhancing secondary products evolution rates.

As observed in primary tar production rate, further increase in temperature above 700 °C did not have any significant effect on the rate of evolution of secondary products from primary tar intra-particle secondary reactions. It is most likely that above 700 °C, primary tar intra-particle secondary reactions were no longer significant to the extent that increase in reactor temperature could barely influence them.

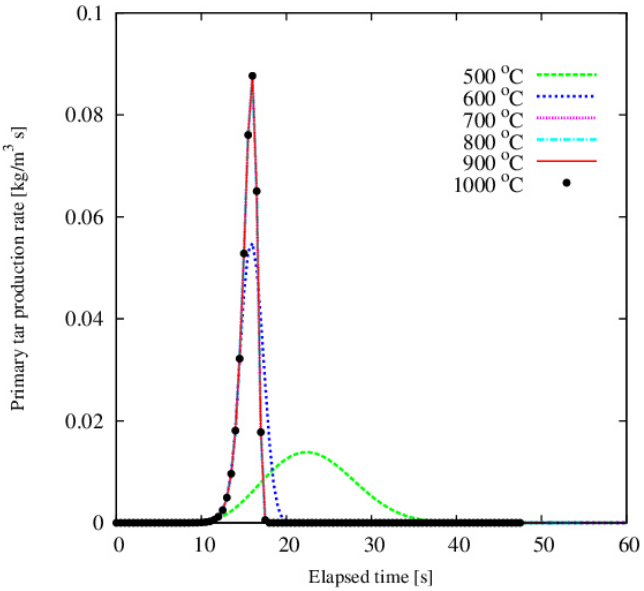

Figure 3: Primary tar production rate at different reactor peak temperatures

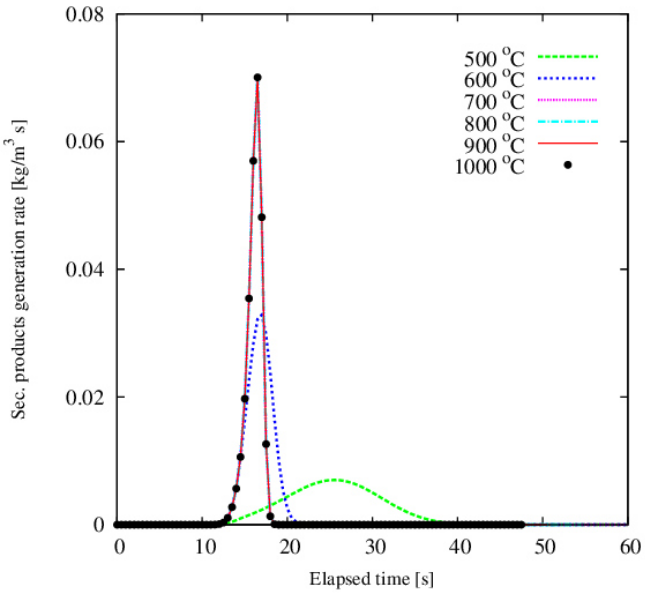

Figure 4: Secondary products evolution at different reactor peak temperatures

4.4 Effect on primary tar release rate

Figure 5 shows primary tar release and consumption rates at different reactor temperatures. From the figure, increase in reactor temperature from 500 to 600 °C increased the rate of primary tar release with the positive peak of the release profile much higher than at 500 °C. The figure also shows that primary tar release rate after reaching its peak at 600 °C began to decline until it became negative and then increased again until it approached

zero, the level it maintained virtually throughout the remaining period of pyrolysis. This scenario left a negative peak which was not observed in thermally thin regime. The negative portion of the profile indicates the rate of consumption of tar molecules as they move through the heated layers within the sample. Some other researchers have reported similar observations [21]. Further increase in reactor temperature from 600 to 700 ^{o}C also caused an increase in the rate of primary tar release. This was also characterized by a negative peak much higher than that at 600 ^{o}C, indicating a higher rate of consumption of primary tar molecules at 700 ^{o}C than at 600 ^{o}C. This is expected to be accompanied with corresponding increase in gas release rate. Temperature increase above 700 ^{o}C had no significant effect on both primary tar release and consumption rates. This suggests that above 700 ^{o}C, sample conversion and intra-particle secondary reactions in the reactor were no longer appreciable, the reason temperature increase could no longer influence the duo.

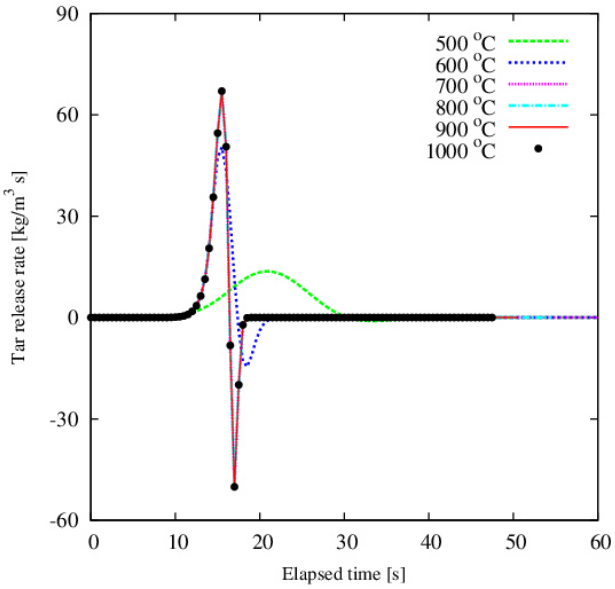

Figure 5: Primary tar release and consumption rates at different reactor peak temperatures

4.5 Effect on gas release rate

Figure 6 shows the rates of gas release at different reactor temperatures. From the figure, as would be expected, gas release rate was lowest at 500 ^{o}C. Temperature increase from 500 ^{o}C to 600 ^{o}C and from 600 ^{o}C to 700 ^{o}C increased the rate of gas release. From chemical kinetics, it is generally believed that increase in temperature accelerates the rate of chemical reactions. Therefore, gas release rate, gas being the main product of volatiles and liquid intra-particle secondary reactions, should be favoured with increase in temperature. Above 700 ^{o}C, increase in temperature had no significant influence on the rate of gas release. This should be expected based on the discussion in section 4.4.

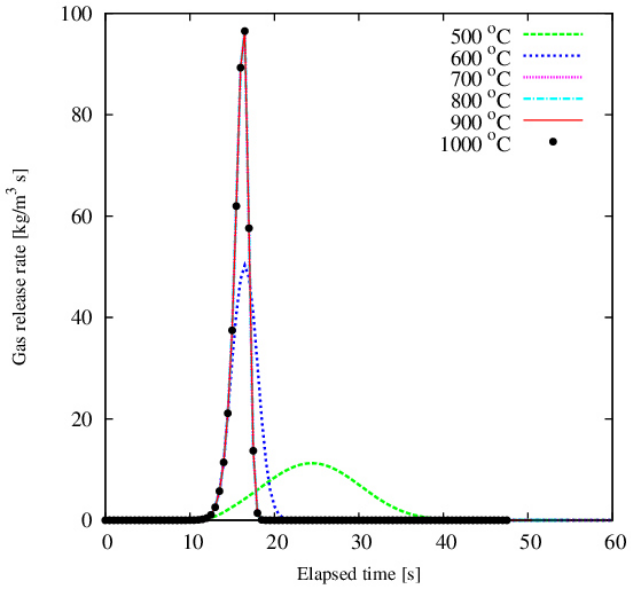

Figure 6: Gas release rates at different reactor peak temperatures

4.6 Effect on intra-particle secondary reactions

Figure 7 shows the ratio of the rate of secondary reactions products generation (R_s) to the rate of primary tar production (R_p) at different reactor temperatures. This ratio is a measure of the degree of intra-particle secondary reactions. From the figure, it is shown that increase in temperature from 500 to 600 ^oC, and from 600 ^oC to 700 ^oC resulted in increase in R_s/R_p. This increase in R_s/R_p value with increase in temperature suggests that intra-particle secondary reactions were favoured. Other researchers have reported that tar cracking is flourished above 600 oC [22]. Further increase in temperature above 700 oC did not affect the ratio Rs/Rp. This kind of result should be expected in the light of sections 4.4 and 4.5.

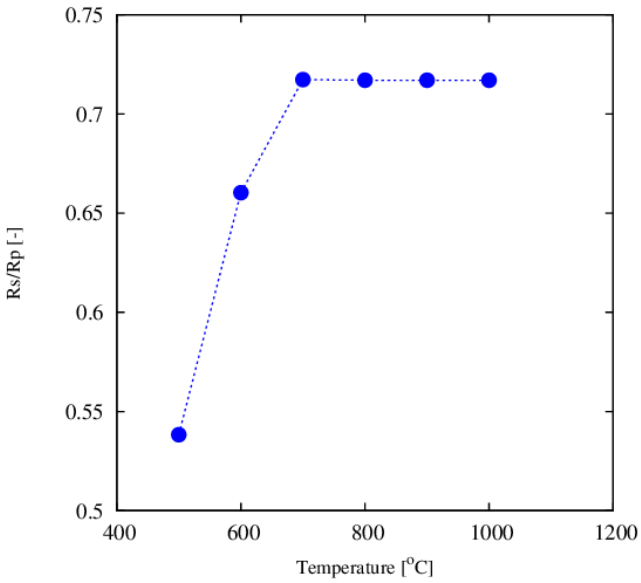

Figure 7: The ratio of the rate of primary tar secondary reactions products generation to the rate of primary tar production at different reactor peak temperatures

4.7 Total product yields

Figure 8 shows the total yield of product species at different reactor temperatures. From the figure, temperature increase from 500 to 600 ^{o}C and from 600 ^{o}C to 700 ^{o}C influenced the yields of primary tar, gas, secondary tar and char. While temperature increase in the two instances increased gas and secondary tar yields, the yield of primary tar and char decreased. It can also be seen from the figure that while further increase in reactor temperature above 700 ^{o}C had no significant effect on the yield of primary tar, secondary tar and gas, char yield continued to decrease with increasing temperature. This is in agreement with the findings of other researchers [23].

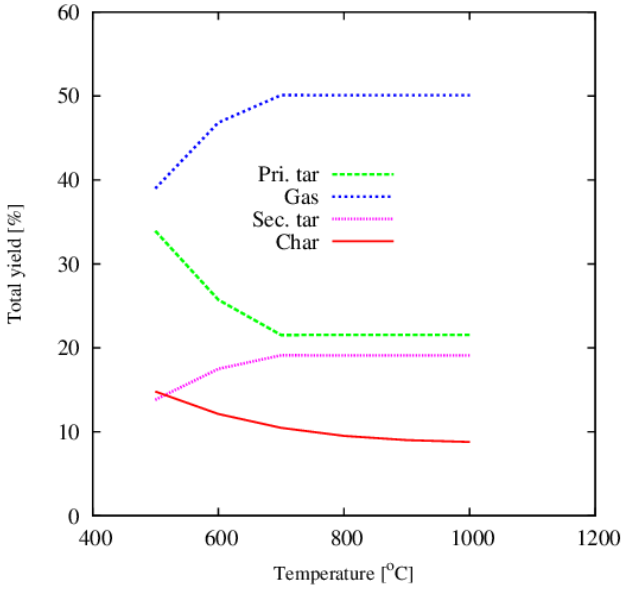

Figure 8: Product yield at different reactor temperatures

As earlier explained, increase in temperature above 700 ^{o}C did not noticeably influence the total yield of primary tar, secondary tar and gas because, above this temperature, both primary degradation of the sample and intra-particle secondary reactions were no longer significant. Depending on the sample size, the level at which temperature increase will no longer influence product distribution may vary.

5. Conclusions

Effect of reactor temperature on product distribution in thermally thick regime during biomass pyrolysis has been investigated under a constant heating rate of 30 K/s and in the temperature range of 500 to 1000 ^{o}C in a fixed bed reactor. Results revealed that increase in reactor peak temperature from 500 to 600 ^{o}C and from 600 to 700 ^{o}C significantly influenced volatiles intra-particle secondary reactions resulting in reduction in primary tar yield and increase in secondary tar and gas yield. Findings also showed that temperature increase above 700 ^{o}C had no significant effect on the yield of primary tar, secondary tar and gas. However, char yield continually declined with increase in temperature. For the considered temperature range, the highest gas yield (50.10%) was obtained at 700 ^{o}C, primary tar yield (33.91%) at 500 ^{o}C, secondary tar (19.11%) at 700 ^{o}C and Char (14.79%) at 500 ^{o}C.

Nomenclature

A: pre-exponential factor	(1/s)
B: permeability	(m^2)
Cp: specific heat capacity	(J/ kg K)
E: activation energy	(J/mol)
e: emissivity	(-)

h_c: convective heat transfer coefficient (W/ m^2 K)
k: reaction rate constant (1/s)
k_c: char thermal conductivity (W/m K)
k_w: wood thermal conductivity (W/m K)
M: molecular weight (kg/mol)
P: Pressure (Pa)
Q: heat generation (W/m^3)
Q_c: convective heat flux (W/m^2)
Q_r: radiation heat flux (W/m^2)
R: universal gas constant (J/mol K)
R: total radial length (m)
r: radial direction
z: axial direction
S: source term
T: temperature (K)
t : time (s)
U: axial velocity component (m/s)
V: radial velocity component (m/s)
ε: porosity (-)
ε_0: initial porosity (-)
Δh: heat of reaction (kJ/kg)
μ: viscosity (kg/m s)
ρ: density (kg/m^3)
ρ_{w0}: initial density of wood (kg/m^3)
σ: Stefan-Boltzmann constant (W/m^2 K^4)
η: degree of pyrolysis

Subscripts
Ar: Argon
c: char, primary char formation reaction
c_2: secondary char formation reaction
g: gas, primary gas formation reaction
g_2: secondary gas formation reaction
is: intermediate solid, intermediate solid formation reaction
s: solid
t: tar, tar formation reaction
v: total volatile
w: wood

References

[1] Scotts, D.S., Piskorz, J., Bergougnou, M.A., Graham, R. & Overend, R.P. (1988). The Role of Temperature in the Fast Pyrolysis of Cellulose and Wood. *Industrial Chemistry Research,* 27, 8-15.
[2] Scott, D.S. & Piskorz, J. (1982). The Flash Pyrolysis of Aspen-poplar Wood. *Canadian Journal of Chemical Engineering,* 60, 666-674. In Modeling Chemical and Physical processes of Wood and Biomass Pyrolysis, Progress in Energy and Combustion Science, 34 (2008), 47-90.
[3] Di Blasi, C. & Branca, C. (2001). Kinetics of primary Product Formation from Wood Pyrolysis. *Industrial Engineering Chemistry Research,* 40, 5547-5556.
[4] Miller, R.S. & Bellan, J. (1996). Analysis of Reaction Products and Conversion Time in the Pyrolysis of cellulose and Wood Particles. *Combustion Science and Technology,* 119, 331-373.
[5] Di Blasi, C. (2008). Modeling Chemical and Physical Processes of Wood and Biomass Pyrolysis. *Progress in Energy and Combustion Science*, 34, 47-90.
[6] Di Blasi, C., Signorelli, G., Di Russo, C. & Rea, G. (1999) Product Distribution from Pyrolysis of Wood and Agricultural Residues. *Industrial Engineering chemistry Research,* 38, 2216-2224.
[7] Liaw, S., Wang, Z., Ndegwa, P., Frear, C., Ha, S. & Li, C. (2012) Effect of Pyrolysis Temperature on the Yield and Properties of Bio-Oils Obtained from the Auger Pyrolysis of Douglas Fir Wood. *Journal of Analytical and Applied Pyrolysis,* 93, 52-62.
[8] Zeng, K., Minh, D.P., Gauthier, D., Weiss-Hortala, E., Nzihou, A. & Flamant, G. (2015). The Effect of Temperature and Heating Rate on Char Properties Obtained from Solar Pyrolysis of Beech Wood, *Bioresource Technology*, 182, 114-119.

[9] Piskorz, J., Radlein D. & Scott, D.S. (1986). On the mechanism of the rapid pyrolysis of cellulose. *Journal of Analytical and Applied pyrolysis,* 9, 121-137.
[10] Graham, R.G., Bergougnou, M.A. & Freel, B.A. (1994). The kinetics of vapor-phase cellulose fast pyrolysis reactions. Biomass & Bioenergy, 7, 33-47.
[11] Hajaligol, M.R., Howard, J.B. & Peters, W.A. (1993). An Experimental and Modeling Study of Pressure Effects on Tar Release by Rapid Pyrolysis of Cellulose Sheets in a Screen Heater, *Combustion and Flame,* 95, 47-60.
[12] Suuberg, E.M., Milosavljevic, L. & Oja, V. (1996). Two-regime global kinetics of cellulose pyrolysis: The role of tar evaporation. Twenty-Sixth Symposium (International) on Combustion/ The Combustion Institute, 1515-1521.
[13] Giudicianni, P., Cardone, G., Ragucci, R. & Cavaliere, A. (2011). Effect of Temperature and Pressure on Steam Pyrolysis of Cellulose. XXXIV Meeting of the Italian Section of the Combustion Institute, 10.4405/34proci2011.III7
[14] Okekunle, P.O. & Osowade E.A. (2014). Numerical Investigation of the Effects of Reactor Pressure on Biomass Pyrolysis in Thermally Thin Regime. *International Journal of Chemical and Process Engineering Research,* 27, 12-22.
[15] Okekunle, P.O., Adeniranye, D.I. & Osowade, E.A. (2014). Numerical Investigation of the Effects of Reactor Pressure on Biomass Devolatilization in Thermally Thick Regime. *International Journal of Chemical and Process Engineering Research,* 28, 1-10.
[16] Okekunle, P.O., Osowade, E.A. & Oyekale, J.O. (2015). Numerical Investigation of the Combined Impact of Reactor Pressure and Heating Rate on Evolution and Yields of Biomass Pyrolysis Products in Thermally Thin Regime. *Journal of Energy Technologies and Policies*, 5(3), 93-106.
[17] Okekunle, P.O. & Adeniranye, D.I. (2015). Effect of Pressure and Heating Rate on Products Release Rates and Yields during Biomass Pyrolysis in Thermally Thick Regime. *Journal of Energy Technologies and Policy*, 5(4), 35-39.
[18] Okekunle, P.O., Watanabe, H., Pattanotai, T. & Okazaki, K. (2012). Effect of Biomass Size and Aspect Ratio on Intra-particle Tar Decomposition during Wood Cylinder Pyrolysis. *Journal of Thermal Science and Technology* 7(1), 1-15.
[19] Okekunle, P.O., Pattanotai, T., Watanabe, H. & Okazaki, K. (2011). Numerical and Experimental Investigation of Intra-particle Heat Transfer and Tar Decomposition during Pyrolysis of Wood Biomass. *Journal of Thermal Science and Technology,* 6(3), 360-375.
[20] Okekunle, P.O. (2013). Numerical Investigation of the Effects of Thermo-physical Properties on Tar Intra-particle Secondary Reactions during Biomass Pyrolysis, *Mathematical Theory and Modeling*, 3(14), 83-97.
[21] Grønli, M.G. & Melaaen, M.C. (2000). Mathematical Model for Wood Pyrolysis - Comparison of Experimental Measurements with Model Predictions. *Energy & Fuel,* 14, 791- 800.
[22] Fagbemi, L., Khezami, L. & Capart, R. (2001). Pyrolysis from Different Biomasses: Application to the Thermal Cracking of Tar. *Applied Energy*, 69, 293-306.
[23] Aysu, T. & Küçük, M.M. (2014) Biomass Pyrolysis in a Fixed-Bed Reactor: Effects of Pyrolysis Parameters on Product Yields and Characterization of Products. *Energy*, 64, 1002-1025.

The IISTE is a pioneer in the Open-Access hosting service and academic event management. The aim of the firm is Accelerating Global Knowledge Sharing.

More information about the firm can be found on the homepage:
http://www.iiste.org

CALL FOR JOURNAL PAPERS

There are more than 30 peer-reviewed academic journals hosted under the hosting platform.

Prospective authors of journals can find the submission instruction on the following page: http://www.iiste.org/journals/ All the journals articles are available online to the readers all over the world without financial, legal, or technical barriers other than those inseparable from gaining access to the internet itself. Paper version of the journals is also available upon request of readers and authors.

MORE RESOURCES

Book publication information: http://www.iiste.org/book/

Academic conference: http://www.iiste.org/conference/upcoming-conferences-call-for-paper/

IISTE Knowledge Sharing Partners

EBSCO, Index Copernicus, Ulrich's Periodicals Directory, JournalTOCS, PKP Open Archives Harvester, Bielefeld Academic Search Engine, Elektronische Zeitschriftenbibliothek EZB, Open J-Gate, OCLC WorldCat, Universe Digtial Library , NewJour, Google Scholar